

Energy transfer, luminescence properties, and thermal stability of color tunable barium pyrophosphate phosphors

Meng-Jiao Xu(徐梦姣), Su-Xia Li(李素霞), Chen-Chen Ji(季辰辰), Wan-Xia Luo(雒晚霞), Lu-Xiang Wang(王鲁香)

Citation: Chin. Phys. B . 2020, 29(6): 063301 . **doi:** 10.1088/1674-1056/ab821a
Journal homepage: http://cpb.iphy.ac.cn; http://iopscience.iop.org/cpb

What follows is a list of articles you may be interested in

Photoluminescence properties of blue and green multiple InGaN/GaN quantum wells

Chang-Fu Li(李长富), Kai-Ju Shi(时凯居), Ming-Sheng Xu(徐明升), Xian-Gang Xu(徐现刚), Zi-Wu Ji(冀子武)

Chin. Phys. B . 2019, 28(10): 107803 . **doi:** 10.1088/1674-1056/ab4046

Spectral properties of Pr:CNGG crystals grown by micro-pulling-down method

Yan-Yan Xue(薛艳艳), Na Li(李纳), Dong-Hua Hu(胡冬华), Qing-Song Song(宋青松), Xiao-Dong Xu(徐晓东), Dong-Hai Wang(王东海), Qing-Guo Wang(王庆国), Dong-Zhen Li(李东振), Zhan-Shan Wang(王占山), Jun Xu(徐军)

Chin. Phys. B . 2019, 28(8): 087801 . **doi:** 10.1088/1674-1056/28/8/087801

Experimental optimum design and luminescence properties of $NaY(Gd)(MoO_4)_2$: Er^{3+} phosphors

Jia-Shi Sun(孙佳石), Sai Xu(徐赛), Shu-Wei Li(李树伟), Lin-Lin Shi(石琳琳), Zi-Hui Zhai(翟梓会), Bao-Jiu Chen(陈宝玖)

Chin. Phys. B . 2016, 25(6): 063301 . **doi:** 10.1088/1674-1056/25/6/063301

Exploring photocurrent output from donor/acceptor bulk-heterojunctions by monitoring exciton quenching

Wang Xin-Ping, He Zhi-Qun, Liang Chun-Jun, Qiu Hai-An, Jing Xi-Ping

Chin. Phys. B . 2015, 24(6): 063301 . **doi:** 10.1088/1674-1056/24/6/063301

Quantitative analysis of the self-absorption and reemission effects on the emission spectrum of photoluminescence in right-angle excitation–detection configuration

Wang Zhen-Hua, Wu Yu-E, Zhang Xin-Zheng, Yun Zhi-Qiang, Li Wei, Xu Jing-Jun

Chin. Phys. B . 2013, 22(11): 113301 . **doi:** 10.1088/1674-1056/22/11/113301

Energy transfer, luminescence properties, and thermal stability of color tunable barium pyrophosphate phosphors*

Meng-Jiao Xu(徐梦姣)[1], Su-Xia Li(李素霞)[1], Chen-Chen Ji(季辰辰)[2], Wan-Xia Luo(雒晚霞)[1], and Lu-Xiang Wang(王鲁香)[1,†]

[1] *Key Laboratory of Energy Materials Chemistry of Ministry of Education, Key Laboratory of Advanced Functional Materials of Xingjiang Uygur Autonomous Region, Institute of Applied Chemistry, Xinjiang University, Urumqi* 830046, *China*

[2] *College of Chemistry and Chemical Engineering, Xinjiang University, Urumqi* 830046, *China*

(Received 15 February 2020; revised manuscript received 9 March 2020; accepted manuscript online 23 March 2020)

A series of barium pyrophosphate $Ba_2P_2O_7$ (BPO) phosphors doped with Ce^{3+} or Tb^{3+} ions is synthesized via a co-precipitation method under reducing atmosphere. The phase structures, photoluminescence (PL) properties, and thermal stabilities of the samples are characterized by using powder x-ray diffraction (PXRD) and PL spectra. The emission colors of samples can be tuned from blue (0.1544, 0.0310) to green (0.2302, 0.4229) by changing the doping concentrations of Tb^{3+} under ultraviolet excitation. The energy transfer mechanism between Ce^{3+} and Tb^{3+} in the BPO is dipole–dipole interaction with a critical distance of 25.86 Å and an energy transfer efficiency of about 85%, which are determined through the PL spectrum and the decay curve. Moreover, the Ce^{3+}/Tb^{3+} co-doped sample has good thermal stability for temperature quenching, and the emission intensity at 423 K is maintained at 95% measured at 298 K. The above results show that the BPO:Ce^{3+}, Tb^{3+} can serve as a promising candidate of green emitting phosphor for solid-state lighting.

Keywords: phosphor, photoluminescence, energy transfer, thermal stability

PACS: 33.50.–j, 78.55.–m, 65.40.–b **DOI:** 10.1088/1674-1056/ab821a

1. Introduction

Inorganic luminescent material is widely used in energy saving lighting, biological medicine, electronic information, military industry, modern agriculture, and other fields. Among these applications, illumination is one of the most important areas where inorganic luminescent material is applied.[1,2] At present, white light emitting diode (w-LED) is considered to be one of the new-generation energy-saving green light sources due to its excellent luminescence performance.[3–5] As a key component of LED, phosphor has also attracted extensive attention. The eventual performance of w-LED device depends mainly on the phosphors, so it is necessary to explore new phosphors that can be effectively excited by ultraviolet/near-ultraviolet (UV/n-UV) LED chips and emit light in different colors. Therefore, finding a novel phosphor that can be activated by a UV/n-UV-chip is an urgent task to be fulfilled.

As is well known, the rare earth ions have been used as the luminescent center in most of inorganic phosphors due to their unique electrical layer structures, stable physical and chemical properties, high absorption energy, and high conversion efficiencies. The Tb^{3+} ions are commonly used to prepare green luminescent materials due to their characteristic $^5D_4$–$^7F_5$ transition peaking at around 544 nm.[6–8] However, the absorption of Tb^{3+} peak in the n-UV region is rather weak and the width is very narrow due to the 4f–4f forbidden transition according to the selection rule. For improving the Tb^{3+} absorption in the n-UV region, one of the effective ways is to utilize the energy transfer from sensitizer ions to activator ions in an appropriate host. The Ce^{3+} as a sensitizer due to its strong excitation band originating from the allowed 4f–5d transitions, can efficiently absorb the UV light and transfer energy to Tb^{3+} in many hosts, for example, $Li_3Sc_2(PO_4)_3$:Ce^{3+}, Tb^{3+}; $Ba_3LaNa(PO_4)_3F$:Ce^{3+}, Tb^{3+}; $Ca_2YZr_2(AlO_4)_3$:Ce^{3+}, Tb^{3+}; $BaLu_6(Si_2O_7)_2(Si_3O_{10})$:$Ce^{3+}$, Tb^{3+}; $LiBaPO_4$:Tb^{3+}, Ce^{3+}; $Ca_3Gd(AlO)_3(BO_3)_4$:Tb^{3+}, Ce^{3+}.[9–14]

$Ba_2P_2O_7$ (BPO), as a novel pyrophosphate candidate for the phosphor host, was reported first by ElBelghitti *et al.*[15] In recent years, the BPO phosphor materials doped with rare earth ions have been investigated extensively because of their stable physical and chemistry properties, low cost, good thermal stability, and environmental friendliness.[16] In the literature, Eu^{2+}-doped $Ba_2P_2O_7$ phosphate and $Ba_2P_2O_7$:Tb^{3+}, Eu^{3+} phosphate were studied by many authors and the crystal structural, photoluminescence properties and mechanisms of these phosphor were reported.[17,18] To the best of our knowledge, the luminescence property and mechanism of BPO:Ce^{3+}/Tb^{3+} phosphor has been rarely reported yet. However, in the present work, the Tb^{3+} co-activated BPO phosphor is prepared by the co-precipitation of the emitting color-tunable Ce^{3+}, and its properties are also investigated. By changing the Tb^{3+} ions' doping concentration, the emission

*Project supported by the Natural Science Foundation of Xinjiang Uygur Autonomous Region, China (Grant No. 2017D01C037).

†Corresponding author. E-mail: wangluxiangxju@163.com

© 2020 Chinese Physical Society and IOP Publishing Ltd

color can be tuned from blue to green light, and the luminescence mechanism of energy transfer and thermal stability are discussed.

2. Experimental section

2.1. Materials and synthesis

A series of BPO:xCe^{3+}, yTb^{3+}, (x = 0.005–0.16, y = 0.00–0.10) samples was synthesized by a co-precipitation method, and the stoichiometric ratio of the desired product weighed $Ba(NO_3)_2$ (that is analytically pure (AR)), $Ce(NO_3)_3{\cdot}6H_2O$ (AR), and $Tb(NO_3)_3{\cdot}6H_2O$ (AR), dissolved in a mixed solution of distilled water. Meanwhile, the $(NH_4)_2HPO_4$ (AR) was slowly added dropwise into the above mixture solution by being dissolved in distilled water and a white precipitate was formed. To complete the reaction, the mixed solution was stirred by a magnetic stirrer for 1 h. The precipitates were filtered, washed with distilled water, and dried for 3 h at 100 °C to obtain a precursor, sequentially. Finally, the precursor was sintered at 1000 °C for 2 h under a reducing atmosphere (N_2/H_2 = 95%/5%), and the samples were cooled to room temperature.

2.2. Characterization

The compositions of the samples were characterized by powder x-ray diffractometer (PXRD, D8 Advance, Bruker, Germany) with Cu-$K\alpha$ radiation at 40 kV and 40 mA. The PL emission and PL excitation (PLE) spectra of barium pyrophosphate phosphors were recorded on a Hitachi F-4500 spectrophotometer equipped with a 150-W Xe light source. The thermal stability and decay curves of samples were performed on a HORIBA JobinYvon Fluorolog-3.

3. Results and discussion

3.1. Phase analysis and crystal structures

Figure 1(a) shows the XRD patterns of BPO:0.01Ce^{3+}, 0.01Tb^{3+}, BPO:0.01Tb^{3+}, BPO:0.01Ce^{3+}, and the standard diffraction lines based on JCPDS card No. 83-0990. All the diffraction peaks of the obtained samples are in good agreement with the standard data of BPO, and no impurity phase peaks are identified. It indicates that there exist a small quantity of doped rare-earth Ce^{3+} and Tb^{3+} ions that do not change the crystal structure. The BPO has been found to have two types of structures: orthorhombic and hexagonal structures.[15,19] The hexagon of the BPO indicates that the sample is in a higher temperature stage. The crystal structure of BPO is shown to have a hexagonal unit cell with a space group P-62m (Fig. 1(b)). The lattice parameters are determined to be a = 9.415 Å, b = 9.415 Å, and c = 7.078 Å. Depending on the coordination environment, the Ba^{2+} cations are divided into two types: one is coordinated by seven oxygen atoms and the other is coordinated by ten oxygen atoms. Ba_1–O and Ba_2–O average bond lengths are in the a range of 2.878 Å–3.080 Å and 2.778 Å–2.869 Å, respectively. The $[P_2O_7]$ group has three axes that pass through two P ions. Based on their effective ionic radii, Ce^{3+} and Tb^{3+} ions occupy the intended radius Ba_1 or Ba_2 site.

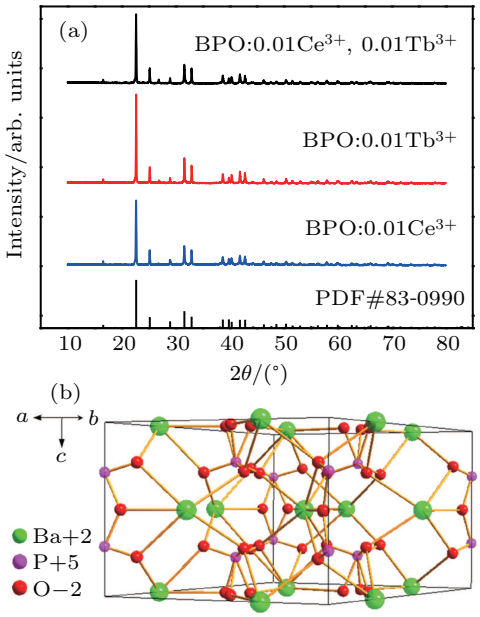


Fig. 1. (a) XRD patterns of BPO:0.01Ce^{3+}, 0.01Tb^{3+}; BPO:0.01Tb^{3+}; BPO:0.01Ce^{3+} and the standard pattern of BPO (JCPDS card No. 83-0990); (b) schematic illustration of crystal structure of BPO.

3.2. Luminescence properties and mechanism

The photoluminescence and photoluminescence excitation spectra of BPO:0.01Ce^{3+}, BPO:0.01Tb^{3+}, and BPO:0.01Ce^{3+}, 0.01Tb^{3+} phosphors are shown in Figs. 2(a)–2(c), respectively. Under the excitation at 315 nm, the emission spectrum of the BPO:0.01Ce^{3+} exhibits an asymmetric broad emission band that ranges from 300 nm to 450 nm with a maximum at about 348 nm. The doublet bands of the emission spectrum are observed to be due to the transitions from the lowest 5d excited state to the $^2F_{5/2}$ and $^2F_{7/2}$ spin–orbit split 4f ground state. Under the monitoring of the wavelength of 348 nm, the PLE spectrum of Ce^{3+} in a range from 200 nm to 300 nm presents a broadband excitation peak, attributable to 4f electronic transitions from the ground state to the different crystal field splittings of excited 5d^1 states of Ce^{3+}. In order to study the effect of doping content on luminescence property, a series of BPO:xCe^{3+} (x = 0.005–0.16) phosphors is synthesized. The inset of Fig. 2(a) shows the intensities of the PL spectra of BPO:xCe^{3+} with different Ce^{3+} doping concentrations. The intensity of emission increases gradually with Ce^{3+} doping content increasing and reaches a maximum value at x = 0.01, after that, it decreases dramatically with the further increase of Ce^{3+} doping concentration, which may be attributed to the concentration quenching effect. Figure 2(b) shows the PL and PLE spectra of the as-prepared

BPO:0.01Tb^{3+} phosphor. Monitored at 545-nm emission, the PLE spectrum displays several narrow weak bands between 280 nm and 400 nm, which can be attributed to f–f transitions. Under the excitation wavelength of 372 nm, the PL spectrum of BPO:0.01Tb^{3+} sample includes the $^5D_4$–^7F_j transitions of Tb^{3+} ions, namely 484 nm ($^5D_4$–$^7F_6$), 545 nm ($^5D_4$–$^7F_5$), and 584 nm ($^5D_4$–$^7F_4$). Obviously, the peak intensity at 545 nm is the highest in the whole the emission spectrum, which can serve as a green emission. The BPO:0.01Tb^{3+} phosphor emission intensity is very weak, since the f–f transition cannot effectively absorb UV light. However, due to the introduction of Ce^{3+} ions, the 5d–4f transition of an electric dipole is allowed to take place, and thus UV light can be strongly absorbed. The dashed lines in Figs. 2(a) and 2(b) indicate that there is an overlap between the PL band of Ce^{3+} and the f–f absorption of Tb^{3+}. According to the formula given by Dexter:[20,21]

$$P_{SA} = 2\pi/h\,|\langle S,A^*|H_{SA}\ \ |S^*,A\rangle\,|^2 \int_{SA} g_S(E)g_A(E)\mathrm{d}E, \quad (1)$$

where P_{SA} is the energy transfer rate, and H_{AS} is the interaction Hamiltonian, the matrix element indicates the interaction between the initial state $|S^*,A\rangle$ and the final state $\langle S,A^*|$; the integral represents the spectral overlap between the PLE spectrum of Tb^{3+} and the PL spectrum of Ce^{3+}. From the observations from Fig. 2(a), Fig. 2(b), and Eq. (1) it can be concluded that the energy transfer can occur from Ce^{3+} to Tb^{3+} in the BPO matrix. This is further confirmed by the PLE and PL spectra of BPO:0.01Ce^{3+}, 0.01Tb^{3+} phosphor in Fig. 2(c). Under the excitation at 315 nm, it is clearly shown that the PL spectrum of BPO:0.01Ce^{3+}, 0.01Tb^{3+} co-doped sample displays both the characteristic Ce^{3+} broad band emission and the Tb^{3+} sharp emission lines. The green emission in BPO:0.01Ce^{3+}, 0.01Tb^{3+} is enhanced compared with that in BPO:0.01Tb^{3+}, which is due to the occurrence of energy transfer from Ce^{3+} to Tb^{3+}.

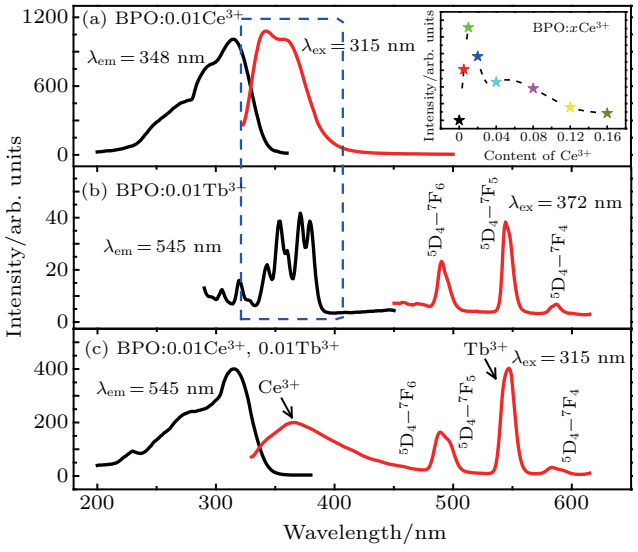


Fig. 2. PL and PLE spectra of (a) BPO:0.01Ce^{3+}, (b) BPO:0.01Tb^{3+}, (c) BPO:0.01Ce^{3+}, 0.01Tb^{3+}. Inset in panel (a) shows variation of emission intensity with Ce^{3+} doping concentration.

A series of Ce^{3+}, Tb^{3+} co-doped phosphors are prepared by varying the Tb^{3+} concentration (y) at a fixed Ce^{3+} concentration of 0.01. Figure 3(a) shows the PL spectra of the BPO:0.01Ce^{3+}, $y$$Tb^{3+}$ (y = 0.00–0.10) phosphors. It can be seen that the emission intensity of Ce^{3+} gradually decreases with Tb^{3+} concentration increasing, whereas the emission intensity of Tb^{3+} gradually increases and then begins to decline after reaching a maximum value at $y = 0.01$ due to concentration quenching. Hence, the optimal composition of Ce^{3+} and Tb^{3+} co-activated phosphor is the BPO:0.01Ce^{3+}, 0.01Tb^{3+}, which shows the strongest green emission. According to Fig. 3(a), figure 3(b) gives the curve of the emission intensity of Ce^{3+} and Tb^{3+} *versus* Tb^{3+} concentration. A change in the doping ion emission intensity can lead the energy transfer process to occur between Ce^{3+} and Tb^{3+}. In order to further understand the detailed information about the energy transfer process between Ce^{3+} and Tb^{3+}, the lifetimes of Ce^{3+} in the BPO:0.01Ce^{3+}, $y$$Tb^{3+}$ (y = 0.00–0.10) are illustrated and calculated in Fig. 3(c). The decay curves of BPO:0.01Ce^{3+}, $y$$Tb^{3+}$ can be well fitted to a single exponential function. The following formula can be obtained:[20–22]

$$I = I_0 \exp(-t/\tau), \quad (2)$$

where I and I_0 are the luminescence intensities at time t and 0, and τ is the decay lifetime. Based on Eq. (2), the lifetime values of Ce^{3+} ions are determined to be 21.03 ns, 10.46 ns, 9.16 ns, 8.85 ns, 8.13 ns, 7.38 ns, and 3.14 ns for the BPO:0.01Ce^{3+}, $y$$Tb^{3+}$ (y = 0.00–0.10) samples. As the content of Tb^{3+} increases, the decay lifetime of Ce^{3+} ions decreases, which proves that there is energy transfer between Ce^{3+} and Tb^{3+} ions in the BPO matrix. The energy transfer efficiency between the Ce^{3+} ions (sensitizer) and the Tb^{3+} ions (activator) is calculated from the decay lifetime through using the following equation:[22–24]

$$\eta_T = 1 - \tau_s/\tau_{so}, \quad (3)$$

where η_T is the energy transfer efficiency, the τ_{so} and τ_s denote the lifetime of the sensitizer Ce^{3+} in the absence and presence of Tb^{3+}, respectively. The dependence of the luminescence lifetime of Ce^{3+} and η_T on Tb^{3+} ion doping concentration are shown in Fig. 3(d). The value of η_T increases gradually with the increase of the Tb^{3+} dopant concentration, and reaches a highest value of 85% at $y = 0.10$, which is higher than those for the reported Ce^{3+}, Tb^{3+} co-doped phosphors such as $Ca_3Al_8Si_4O_{17}N_4$:Ce^{3+}, Tb^{3+} (63.2%),[25] and $Ca_8MgLu(PO_4)_7$:Ce^{3+}, Tb^{3+} (74%).[26]

As is well known, the energy transfer mechanism can be attributed to exchange interaction or electric multipolar interaction. To determine which interaction dominates in the energy transfer process, the critical distance (R_c) between the Ce^{3+} ion and the Tb^{3+} ion is evaluated in the BPO phosphor.

Based on the theory of Blasse, R_c can be estimated according to the following equation:[24–26]

$$R_c = 2\left(\frac{3V}{4\pi\chi_c N}\right)^{1/3}, \tag{4}$$

where N is the number of ions that can be substituted into the unit cell, V is the unit cell volume, and χ_c is the total concentration of Ce^{3+} and Tb^{3+} at the time of concentration quenching. In the BPO host, $V = 543.35$ Å^3, $N = 3$, and $\chi_c = 0.02$. Thus, the corresponding R_c is estimated as approximately 25.86 Å. Generally, this critical distance is greater than 5 Å, indicating that the energy transfer between Ce^{3+}–Tb^{3+} is achieved by electric multipolar interaction. Based on the theory of Van Uitert, the relationship between emission intensity (I) and doping concentration (x) meets the following equation:[27,28]

$$\left(\frac{I}{x}\right) = K\left[1+\beta(x)^{Q/3}\right]^{-1}, \tag{5}$$

where I/x is the emission intensity per activator concentration, x is the activator concentration, K and β are constants for the same excitation condition for a given host crystal, Q represents the interaction type between rare earth ions, here $Q = 6$, 8, 10, which are corresponding to dipole–dipole (d–d), dipole–quadruple (d–q), and quadruple–quadruple (q–q) interactions, respectively. The plot of $\log(I/x)$ as a function of $\log x$ in BPO:0.01Ce^{3+}, $y$$Tb^{3+}$ ($y = 0.00$–0.10) phosphors is shown in Fig. 4. The relation between $\log(I/x)$ and $\log(x)$ is found to be approximately linear and the slope is about -1.9312, then the Q is calculated approximately to be 6. This suggests that the major mechanism for concentration quenching in BPO:0.01Ce^{3+}, $y$$Tb^{3+}$ is a dipole–dipole interaction.

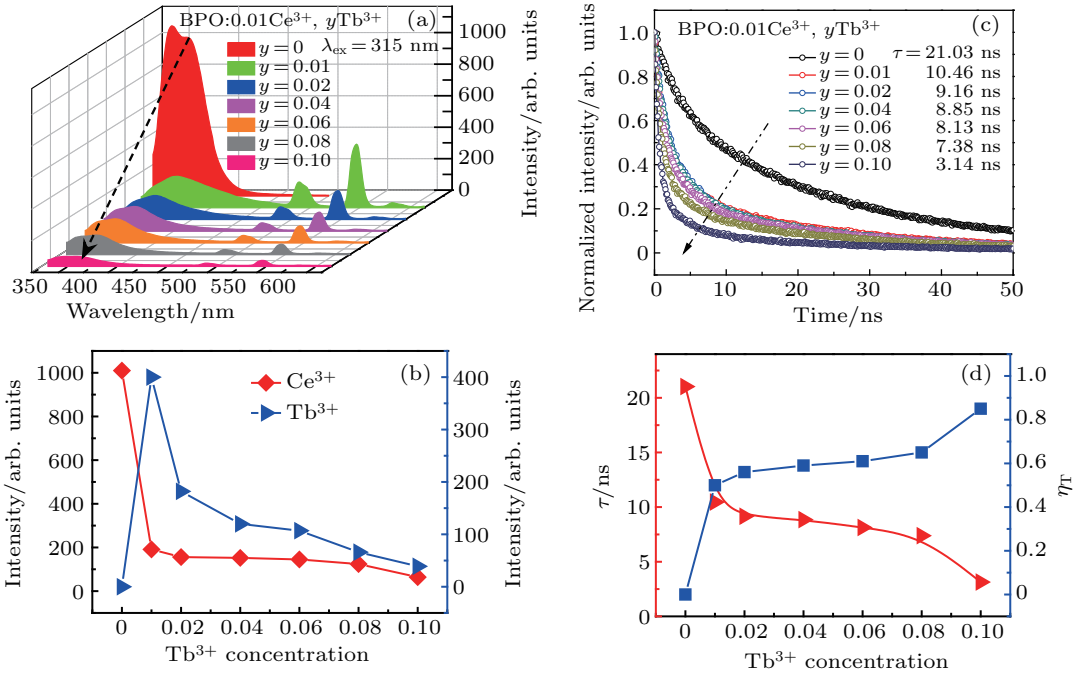


Fig. 3. (a) PL spectra of a series of BPO:0.01Ce^{3+}, $y$$Tb^{3+}$ ($y = 0.00$, 0.01, 0.02, 0.04, 0.06, 0.08, and 0.10) under 315-nm excitation; (b) the intensity of Ce^{3+} at 348 nm and Tb^{3+} at 545 nm varying with Tb^{3+} doping concentration; (c) decay curve of BPO:0.01Ce^{3+}, $y$$Tb^{3+}$ ($x = 0.00$–0.10) recorded under 290-nm nano-LED light; (d) luminescence lifetime of Ce^{3+} and energy transfer efficiency varying with doped Tb^{3+} ion concentration.

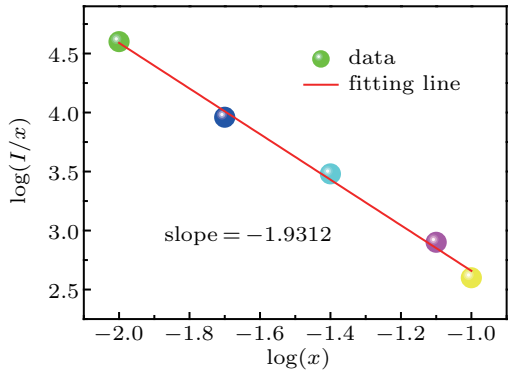


Fig. 4. Relationship between $\log(I/x)$ and $\log(x)$ of BPO:0.01Ce^{3+}, $y$$Tb^{3+}$ ($y = 0.00$–0.10) phosphors.

The Commission International de L' Eclairage (CIE) chromaticity coordinates and the photo images of BPO:0.01Ce^{3+}, $y$$Tb^{3+}$ ($y = 0.00$–0.10) samples upon 315-nm and 245-nm excitations are obtained, and the results are shown in Fig. 5(a). The CIE chromaticity coordinates of BPO:0.01Ce^{3+}, $y$$Tb^{3+}$ shift from $(0.1544, 0.0310)$ to $(0.2302, 0.4229)$ with Tb^{3+} concentration increasing from $y = 0$ to 0.01. Accordingly, the emitting color gradually varies from blue to green with the increase of Tb^{3+} concentration based on the effect of energy transfer from Ce^{3+} to Tb^{3+} ions in the BPO hosts. In addition, the energy level scheme of BPO:Ce^{3+}, Tb^{3+} is used to better understand the energy transfer process (seen Fig. 5(b)). When the Ce^{3+} ions absorb

UV light, the excitation energy can not only emit blue light but also be released by the energy transfer process from Ce^{3+} to Tb^{3+} ions, which can enhance the green emission efficiently.

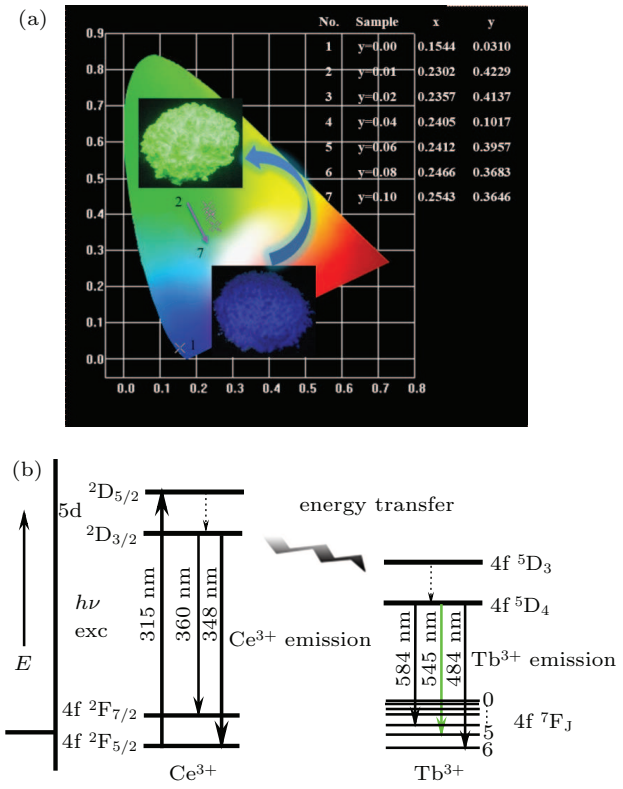


Fig. 5. (a) CIE chromaticity diagram and picture of BPO:0.01Ce^{3+}, $y$$Tb^{3+}$ (y = 0.00–0.10) under 315-nm excitation and a 254-nm UV lamp, respectively, and (b) schematic energy level diagram of Ce^{3+} and Tb^{3+} in the BPO host.

3.3. Thermal stability

For high power LEDs, the thermal stability of the phosphor is a very important performance parameter. Therefore, it is important to study the dependence of the luminescence property of material on temperature. To investigate the influence of temperature on luminescence intensity, the temperature-dependent PL emission spectra (77 K–473 K) of green-emitting phosphor BPO:0.01Ce^{3+}, 0.01Tb^{3+} under 315-nm excitation are obtained and displayed in Fig. 6(a). The results indicate a weak decrease in emission intensity of Ce^{3+} and Tb^{3+} with temperature increasing from 298 K to 473 K due to thermal quenching via phonon interaction. Figure 6(b) shows the detailed tendency of the emission intensity varying with temperature. It can be seen that the PL intensity just decreases to 95% of the initial intensity (298 K) at 423 K. For the temperature quenching phenomenon, it is explained by configuration coordinate model as shown in Fig. 6(c). In Fig. 6(c), the electron intersects the ground state curve and the excited state curve at point T. When the temperature is high enough, the electrons in the excited state at point B are likely to absorb more energy to arrive at point T. However, T is both an excited state and a ground state, so it is possible for the electrons go back to point A along the T–D–A curve. In this process, the system returns from the excited state without radiation to the ground state equilibrium point, which is the quenching phenomenon of temperature.

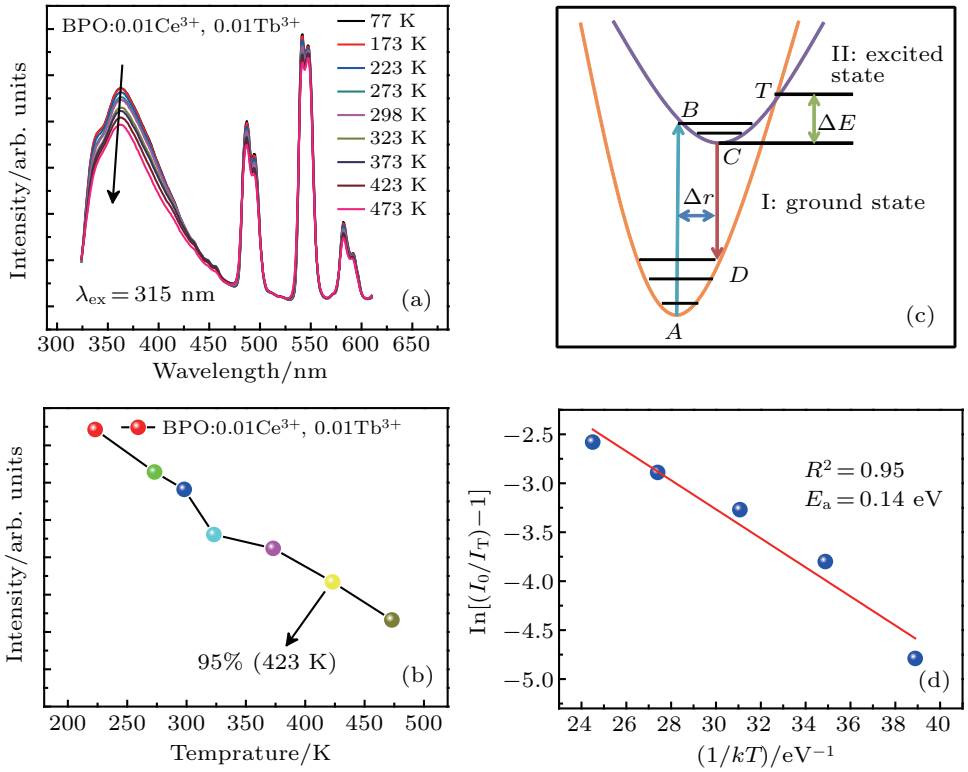


Fig. 6. (a) Temperature-dependent PL spectra of the BPO:0.01Ce^{3+}, 0.01Tb^{3+} under 315-nm excitation; (b) normalized intensity *versus* temperature; (c) schematic configuration coordinate model; (d) plot of $\ln[(I_0/I)-1]$ *versus* $1/kT$.

The activation energy (E_a) is another parameter to evaluate the thermal stability performance of the as-prepared phosphor. The E_a can be acquired from the following formula proposed by Arrhenius:[29,30]

$$\ln\left(\frac{I_0}{I}\right) = \ln A - \frac{E_a}{kT}, \tag{6}$$

where I_0 is the initial luminescence intensity, I is the luminescence intensity at different test temperatures, E_a is the activation energy, k is the Boltzmann constant ($k = 8.626 \times 10^{-5}$ eV/K), and T is the temperature. The curve of $\ln[(I_0/I) - 1]$ *versus* $1/kT$ of the BPO:0.01Ce^{3+}, 0.01Tb^{3+} phosphor is illustrated in Fig. 6(d). E_a can be extracted from the slop of the plot. The value of E_a was calculated to be 0.14 eV, which is close to the commercial phosphor YAG:Ce^{3+} ($E_a = 0.136$ eV) phosphor.[31]

4. Conclusions

In summary, BPO:Ce^{3+}, Tb^{3+} phosphors are synthesized successfully via the co-precipitation method followed by calcination at 1000 °C for 2 h in a 95%N_2–5%H_2 atmosphere. The luminescence properties and energy transfer behavior of the BPO:Ce^{3+}, Tb^{3+} are investigated in detail. The color of the obtained phosphors can turn from blue to green by adjusting the relative doping concentration of Ce^{3+} and Tb^{3+} ions in the BPO host. By fluorescence spectrum and life decay curve, the Ce^{3+} and Tb^{3+} ion experience the dipole–dipole interaction during energy transfer in the BPO host, and the energy transfer efficiency can reach 85%, and the critical distance is calculated to be 25.86 Å according to the concentration quenching method. The novel BPO:Ce^{3+}, Tb^{3+} phosphors have excellent thermal stability and luminescence properties. So, it is clear that the novel BPO:Ce^{3+}, Tb^{3+} phosphors exhibit high potential as phosphors in phosphor converted white light n-UV LEDs.

References

[1] Lin C C and Liu R S 2011 *J. Phys. Chem. Lett.* **2** 1268
[2] Hoppe H A 2009 *Angew. Chem. Int. Ed. Engl.* **48** 3572
[3] Zhou J, Liu Q L and Xia Z G 2018 *J. Mater. Chem. C* **6** 4371
[4] Zhang B Y, Ying S T, Wang S P, Han L, Zhang J S and Chen B J 2019 *Inorg. Chem.* **58** 4500
[5] Xu S, Wang Z, Li P, Li T, Bai Q, Sun J and Yang Z 2017 *RSC. Adv.* **7** 19584
[6] Li J, Li J G, Li X and Sun X 2016 *Opt. Mater.* **62** 328
[7] Wu Y, Zhu L and Mao H 2018 *Ceram. Int.* **44** 10015
[8] Zhang Z W, Zhong H, Yang S S and Chu X J 2017 *J. Alloys Compd.* **708** 671
[9] Jiao M M, Xu Q F, Liu M L, Yang C L and Yu Y J 2018 *Phys. Chem. Chem. Phys.* **20** 26995
[10] Sun L L, Devakumar B, Liang J, Wang S Y, Sun Q and Huang X Y 2019 *J. Mater. Chem. C* **7** 10471
[11] Lai H L, Yang R Y and Chang S J 2017 *Ceram. Int.* **43** S688
[12] Ma X X, Zhou W, Zhang Z, Wang X R, Zhang B and Guo Y C 2018 *J. Lumin.* **199** 82
[13] Li B, Sun Q, Wang S, Guo H and Huang X 2018 *RSC. Adv.* **8** 9879
[14] Li K, Lian H Z, Han Y, Shang M M, Van R and Lin J 2017 *Dyes Pigments.* **139** 701
[15] ElBelghitti A A, Elmarzouki A, Boukhari A and Holt E M 1995 *Acta Cryst. C* **51** 1478
[16] Kolaya S, Basua M, Sudarsana V and Tyagi A K 2018 *Solid State Sci.* **85** 26
[17] Nakagawa H, Kim S W, Hasegawa T, Hasegawa S, Ishigaki T, Uematsu K, Toda K, Takabad H and Sato M 2017 *Inorg. Chem. Front.* **4** 1562
[18] Wang B X, Ren Q, Hai O and Wu X L 2017 *RSC. Adv.* **7** 15222
[19] Zakaria D, Erragh F, Oudahmane A, E I-Ghozzi M and Avignant D 2010 *Acta Cryst. E* **66** i76
[20] Dexter D L 1953 *J. Chem. Phys.* **21** 836
[21] Blasse G 1986 *J. Solid. State. Chem.* **62** 207
[22] Dexter D L and Schulman J H 1954 *J. Chem. Phys.* **22** 1063
[23] Guo B, Zhang Z W, Jiang D G, Li Y N and Sun X Y 2019 *J. Lumin.* **206** 244
[24] Bian L, Wang T, Song Z, Liu Z H, Li J X and Liu Q L 2013 *Chin. Phys. B* **22** 077801
[25] Lü W, Huo J S, Feng Y, Zhao S and You H P 2016 *Dalton Trans.* **45** 9676
[26] Mi X Y, Sun J C, Zhou P, Zhou H Y, Dong D, Li K, Shang M M and Lin J 2015 *J. Mater. Chem. C* **3** 4471
[27] Ozawa L and Jaffe P M 1971 *J. Electrochem. Soc.* **118** 1678
[28] Blasse G 1968 *Phys. Lett. A* **28** 444
[29] Shang M M, Liang S S, Lian H Z and Lin J 2017 *Inorg. Chem.* **56** 6131
[30] Zhou J and Xia Z G 2014 *J. Mater. Chem. C* **2** 6978
[31] Zhang Y F, Li L, Zhang X S and Xi Q 2008 *J. Rare Earth* **26** 446